Investigating Storm Time Variability of Exospheric Hydrogen with WACCM-X & Lyao_rt

Lauren T. Ashworth[1] (ashwortl@my.erau.edu), Edwin J. Mierkiewicz[1], Liying Qian[2], Joseph M. McInerney[2], Susan M. Nossal[3], R. Carey Woodward[3], & L. Matthew Haffner[1]

[1]Embry-Riddle Aeronautical University, Daytona Beach, FL; [2]High Altitude Observatory, National Center for Atmospheric Research, Boulder, CO; [3]University of Wisconsin-Madison, Madison, WI

Introduction

Previous studies have shown that the terrestrial hydrogen exosphere exhibits significant storm-time variability, driven by geomagnetic forcing and associated thermospheric heating (e.g., Zoennchen et al., 2017; Cucho-Padin & Waldrop, 2019). More recent modeling efforts have combined a global exosphere model with spacecraft Lyman-α observations to investigate these variations in greater detail (Connor et al., 2024). Geomagnetic storms can significantly alter upper atmospheric temperature and density structure, leading to changes in hydrogen scale height and global redistribution of the exosphere. Despite these advances, storm-time changes in hydrogen remain difficult to fully characterize due to the limited spatial and temporal coverage of observations, particularly for ground-based geocoronal Balmer-α (Hα) measurements, which provide only line-of-sight (LOS) integrated information. In this study, we use WACCM-X coupled with the radiative transport code, lyao_rt (Bishop, 1999), to compute Hα column emission intensity during the 6–7 April 2000 geomagnetic storm. This storm was chosen because there exist near-simultaneous ground-based Fabry-Perot interferometer (FPI) observations of Hα from Pine Bluff Observatory (PBO) in Wisconsin. These observations were obtained on 5-6 April 2000 with a maximum $F_{10.7}$ and Ap index of 195 and 82, respectively, at the PBO geographic location. Although the observational coverage is limited, we compare the forward modeled WACCM-X Hα column emission intensities with the near-simultaneous PBO observations of geocoronal Hα providing a means to assess storm-time variability in the modeled neutral thermosphere and resulting Hα emission.

April 2000 Geomagnetic Storm

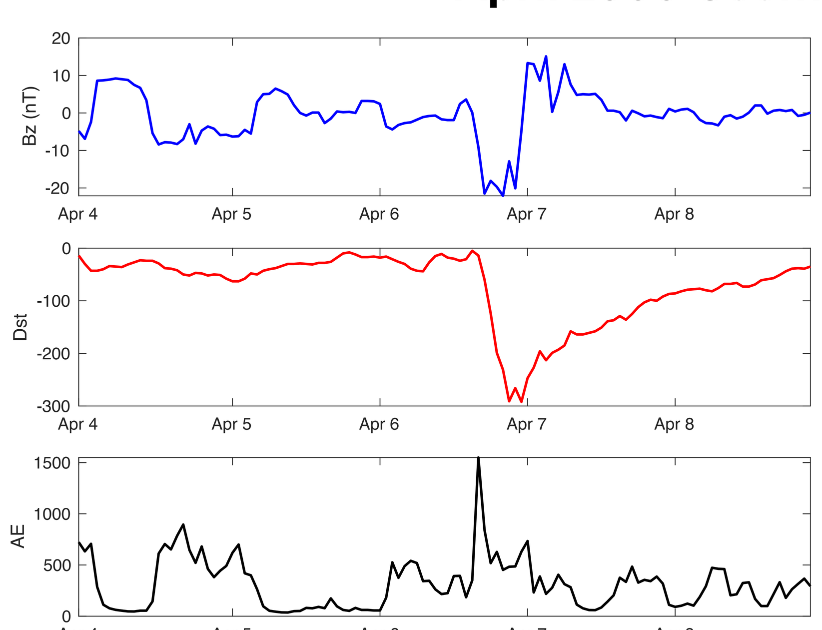

Figure 1 – 6-7 April 2000 Geomagnetic Storm: The storm's main phase (~18 UT on 6 April to ~01 UT on 7 April) is marked by a strong southward IMF Bz, enhanced auroral activity (AE), and a rapid decrease in Dst to −288 nT.

- The 6-7 April 2000 storm reached a Dst of −288 nT, driven by sustained southward IMF during Solar Cycle 23's rising phase.
- The main phase occurred from 18 UT, 6 April to 01 UT, 7 April as characterized by a sustained southward IMF (Bz < 0).
- Strong auroral energy input, denoted by the elevated AE index, produced significant Joule heating in the high latitude thermosphere, increasing neutral temperature.
- Thermospheric heating during the main phase increases scale height, causing global expansion of the neutral atmosphere.
- This event provides a valuable case study due to the availability of near-simultaneous ground-based PBO FPI observations of geocoronal Hα.

Forward Model Description

When coupled with WACCM-X, lyao_rt...

uses WACCM-X thermospheric H density and temperature profiles as inputs. ⇨ Extends WACCM-X hydrogen density to exospheric altitudes using the evaporative case of the Bishop Analytic Exosphere (1991). ⇨ Uses the extended hydrogen density profile and observational viewing geometry to calculate LOS Hα emission intensities.

Forward Model Setup

Exosphere
- Bishop Analytic Exosphere (1991) is used assuming a spherically symmetric, evaporative exosphere.

Solar Input
- Because of high solar activity in the year 2000, the Lyman-β line center flux used here is 14.0 x 10^9 ph cm^{-2} s^{-1} $Å^{-1}$.

Viewing Geometry
- 6 April 2000 observational viewing geometry used for near-simultaneous comparisons.

Temporal Sampling
- Although the observations span the entire night, lyao_rt is evaluated for one AM time (6 AM LT/12 UT) and one PM time (12 PM LT/00 UT).

WACCM-X Hydrogen Density & Temperature

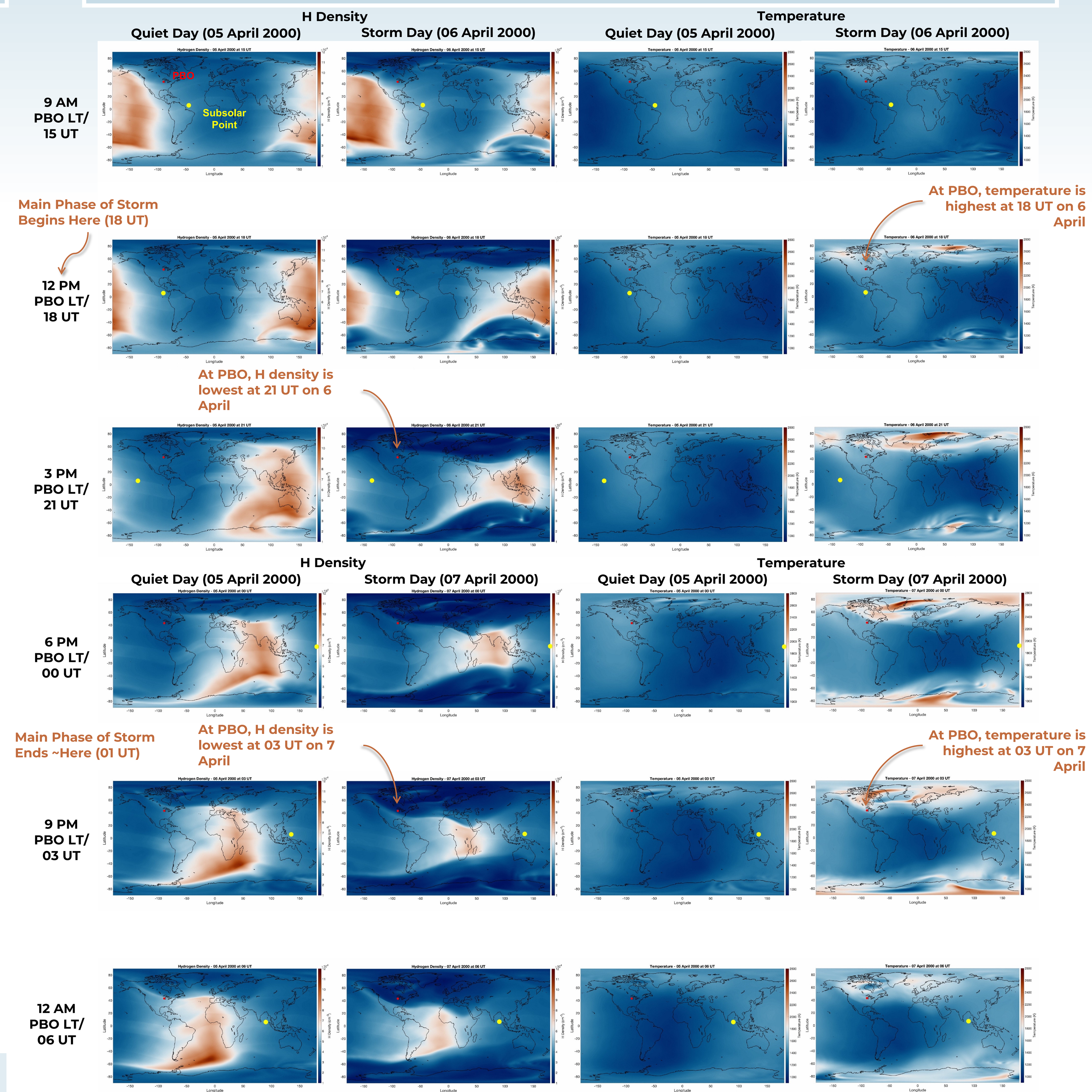

Figure 2 – WACCM-X Global H Density & Temperature: WACCM-X global hydrogen density and temperature at 500 km during the 6–7 April 2000 geomagnetic storm. Results are shown for 15, 18, 21, 00, 03, and 06 UT. The first two columns show H density for **(left)** the quiet reference day (5 April 2000) and **(right)** storm day (6–7 April 2000), while the last two columns show temperature for **(left)** the quiet day and **(right)** storm day. The main phase of the storm occurs from ~18 UT on 6 April to ~01 UT on 7 April. The PBO location is marked with a red dot, and the subsolar point is indicated with a yellow dot. During the main phase of the geomagnetic storm, WACCM-X shows enhanced thermospheric temperatures and reduced H densities at 500 km relative to quiet conditions, indicating strong storm-driven redistribution of the neutral upper atmosphere.

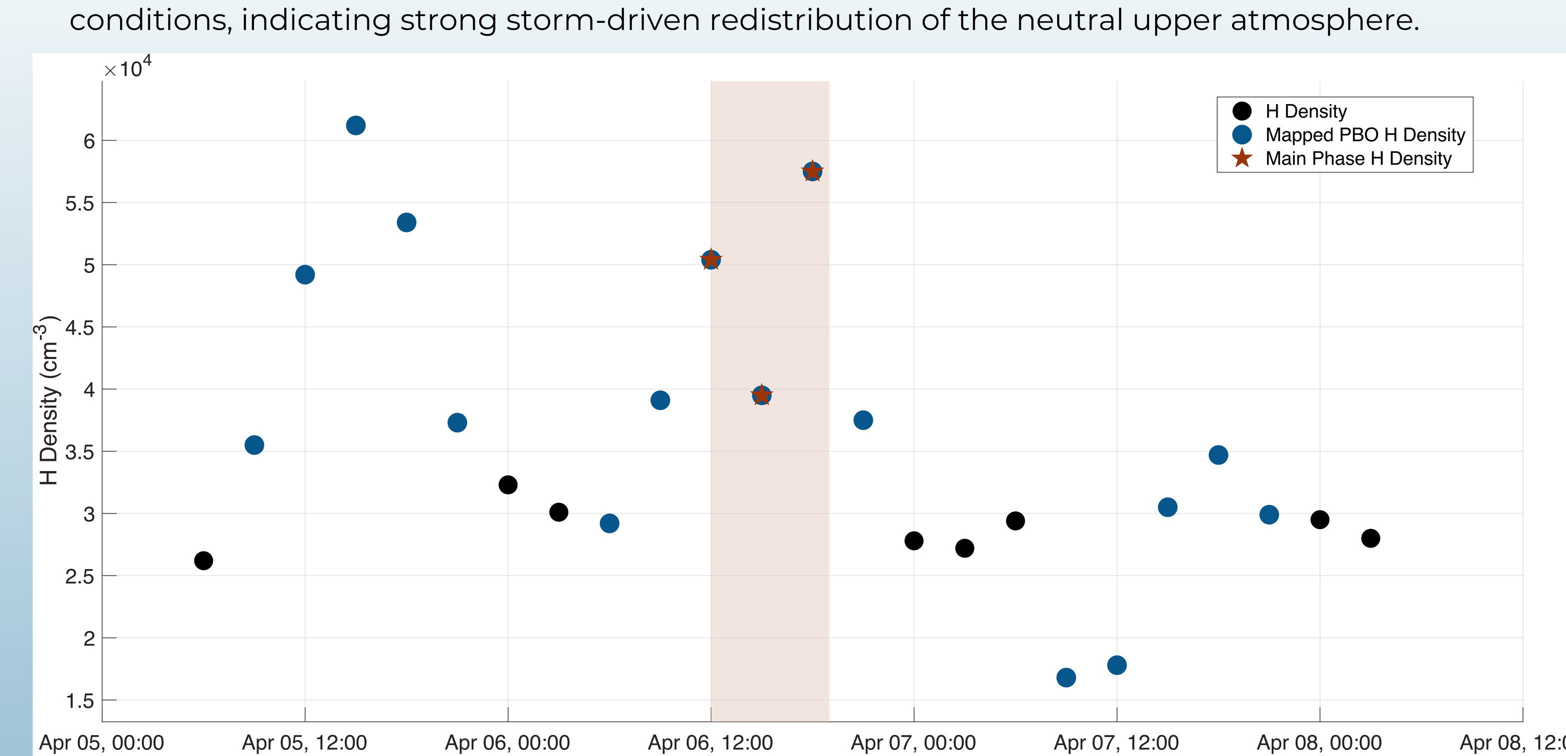

Figure 3 – Diurnal Variation in WACCM-X H Density: WACCM-X simulated H density at 500 km above PBO for 5-7 April 2000. Black circles: H densities not shown in above maps; blue circles: H densities shown in maps; red pentagons: main-phase storm H densities (18 UT 6 April-01 UT 7 April).

Hα Intensity Model-Data Comparison

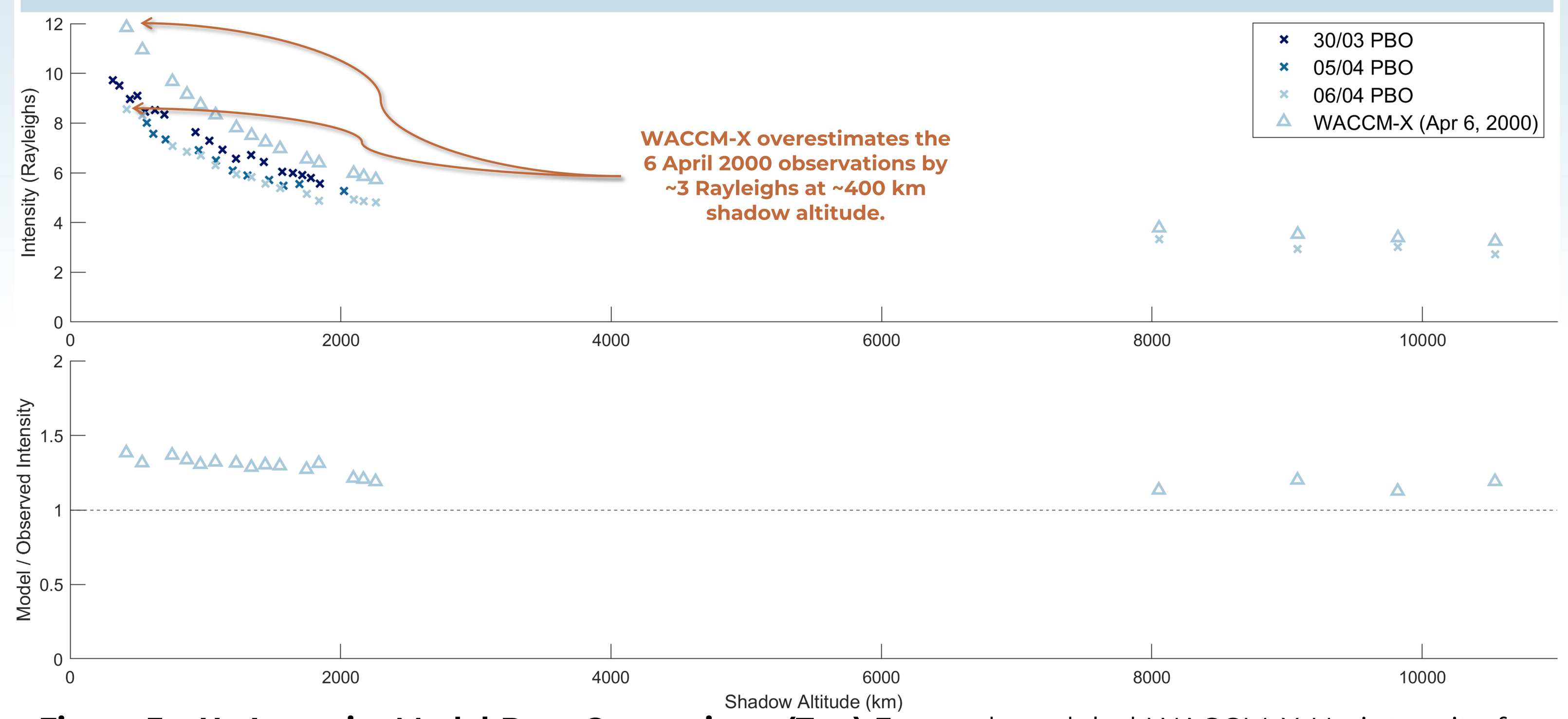

Figure 3 – Hα Intensity Model-Data Comparison: (Top) Forward modeled WACCM-X Hα intensity for pre-storm conditions (12-6 AM LT on 6 April 2000 at PBO) compared to Series 4 observations (3 individual nights). Only forward modeled WACCM-X Hα intensities are presented for 6 April 2000. **(Bottom)** Modeled-to-observed intensity ratio between 6 April 2000 WACCM-X results and the 6 April 2000 observations. Viewing geometry representative of the 6 April 2000 PBO observations and a value of 14.0 x 10^9 ph cm^{-2} s^{-1} $Å^{-1}$ for the solar Lyman-β line center flux are used.

lyao_rt: Probing Detectability of Longitudinal Effects

- **Fixed Viewing Geometry**
  - Zenith viewing geometry is defined at PBO (43.07°N, 89.67°W).
- **Longitude-Dependent WACCM-X Thermospheric Inputs**
  - Nine WACCM-X thermospheric states are selected across 3 different geographic longitudes: 15°W of PBO (43.07°N, 104.67°W), PBO (43.07°N, 89.67°W), and 15°E of PBO (43.07°N, 74.67°W) providing a different H density and temperature background.
- **lyao_rt Simulations**
  - lyao_rt is run using the fixed PBO zenith geometry and PBO coordinates at 06, 09, and 12 UT (spanning 11pm-7am LT) with different WACCM-X thermospheric backgrounds to reflect combined effects of UT-dependent evolution and longitudinal structure in the thermospheric background.

Discussion & Future Work

- From Figure 2, WACCM-X predicts and **inverse relationship between H density and temperature**. This is consistent with diurnal and seasonal variability in the thermosphere where cooler temperatures correspond to higher morning and winter H density.
- In Figure 3, the storm appears to distort the diurnal H density cycle during the main phase and leaves a measurable suppression during recovery, showing a detectable, **multi-day departure from quiet-time behavior in WACCM-X's simulated exospheric H density**.
- From Figure 4, we evaluate the pre-storm thermospheric H density distribution in WACCM-X by comparing forward-modeled Hα column emission intensities with observations. The modeled-to-observed intensity ratio indicates that **WACCM-X overestimates the 6 April 2000 observations by less than a factor of ~1.5 Rayleighs**.
- This work **establishes model validation before the onset of the storm** and motivates future simulations that **extend WACCM-X/lyao_rt through the evening LT (6 PM-12 AM at PBO)**, covering the latter portion of the storm's main phase and into the recovery phase.
- Other future work includes **evaluating simulations of other geomagnetic storm events** and conducting potential comparisons with more recent ground-based FPI observations.

References

Bishop, J. (1991). Analytic exosphere models for geocoronal applications. *Planetary and Space Science* 39, 885–893. doi:10.1016/0032-0633(91)90093-P.

Bishop, J. (1999). Transport of Resonant Atomic Hydrogen Emissions in the Thermosphere and Geocorona: Model Description and Applications. *J. Quant. Spectrosc. Radiat. Transfer*, 61, 4, 473—491.

Connor, H. K., Jung, J., Qian, L., Sutton, E. K., Cucho-Padin, G., Crow, M., & Lee, S.-Y. (2024). Storm-time variability of terrestrial hydrogen exosphere: Kinetic simulation results. *Frontiers in Astronomy and Space Sciences*, *11*, 1421196. doi:10.3389/fspas.2024.1421196.

Cucho-Padin, G., & Waldrop, L. (2019). Time-Dependent Response of the Terrestrial Exosphere to a Geomagnetic Storm. *Geophysical Research Letters*, *46*(21), 11661–11670 doi:10.1029/2019GL084327.

Mierkiewicz, E. J., F. L. Roesler, and S. M. Nossal (2012). Observed seasonal variations in exospheric effective temperatures. *J. Geophys. Res*, 117, A06 313. doi:10.1029/2011JA017123.

Zoennchen, J. H., Nass, U., Fahr, H. J., & Goldstein, J. (2017). The response of the H geocorona between 3 and 8 R_e to geomagnetic disturbances studied using TWINS stereo Lyman-α data. *Annales Geophysicae*, *35*(1), 171–179. doi:angeo-35-171-2017.

Acknowledgments

This work is supported by NSF CEDAR AGS-2050077, NSF CEDAR AGS-2049536, and NSF CEDAR AGS-2050072, a collaborative effort between ERAU, UW-Madison, UC-Boulder, and NSF NCAR. The authors would like to give a special thanks to the late James Bishop for the development, implementation, and use of the lyao_rt code.